Lifetime of the Histone Octamer Studied by Continuous-Flow Quasielastic Light Scattering: Test of a Model for Nucleosome Transcription†

H.-P. Feng, Dale S. Scherl, and J. Widom*

Department of Biochemistry, Molecular Biology, and Cell Biology and Department of Chemistry, Northwestern University, Evanston, Illinois 60208-3500

Received March 15, 1993; Revised Manuscript Received April 28, 1993

ABSTRACT: An instrument for continuous-flow quasielastic light scattering is described that allows the translational diffusion coefficient of macromolecules to be determined as a function of time after the initiation of some time-dependent process by mixing. Control experiments are carried out using the proteins lysozyme and BSA to verify that flow of the solution does not lead to erroneous results. The instrument is used to determine the lifetime of the histone octamer. A solution of octamer that is artificially stabilized in 2.0 M NaCl is rapidly diluted to physiological ionic strength, and the Stokes diameter is determined as a function of the time, Δt, after mixing. We find that the octamers dissociate into their component H2A–H2B heterodimers and $H3_2H4_2$ tetramers on a time scale that is faster than the earliest time point for which data were obtained, 1 s after mixing. This result argues against a simple mechanism for the progression of RNA or DNA polymerase through chromatin.

Quasielastic light scattering (QLS)[1] is a rapid and sensitive technique for measurement of translational diffusion coefficients of biological macromolecules and macromolecular assemblies (Berne & Pecora, 1976; Bloomfield & Lim, 1978; Chu, 1974; Pecora, 1985). Diffusion coefficients are extracted by fitting the time-decay of the measured intensity autocorrelation function to a model. Results for compact macromolecules are commonly represented in terms of the radius or diameter of a hydrodynamically equivalent sphere, known as the Stokes radius or diameter. Samples consisting of a distribution of molecular sizes can, in favorable cases, be analyzed to yield the distribution. QLS is ideally suited to measuring conformational changes that affect size, including those associated with folding and unfolding, and to measuring changes in the oligomeric state.

QLS can also be used in kinetic studies. However, an essential limitation in any such study is that one must signal-average the scattering intensity autocorrelation function for a relatively long period, typically tens of seconds to tens of minutes, in order to obtain an adequate signal to noise ratio. Two limiting cases for the application of QLS to kinetically evolving systems have previously been analyzed (Berne & Pecora, 1976; Bloomfield & Lim, 1978). In one limit, the time scale of a process is long compared to the time required to make a QLS measurement. One example is a QLS study of the joining of bacteriophage heads with tails, a bimolecular reaction. Despite the large rate constant for this reaction ($\sim 1 \times 10^7\ M^{-1}\ s^{-1}$), simply by diluting the system the reaction rate could be brought into an appropriate time scale; the reaction was conveniently followed by taking successive measurements, each 40 s in duration, over a period of $\sim$1 h (Aksiyote-Benbasat & Bloomfield, 1975, 1981; Bloomfield & Lim, 1978). This experiment was possible chiefly because of the very great sensitivity of QLS for scatterers having sufficiently large molecular weight, such as bacteriophage capsids (MW $\sim 1.8 \times 10^8$), allowing diffusion coefficients to be measured with extraordinarily low molar concentrations of scatterers. A second limiting case accessible to QLS is that of rapid dynamic equilibrium. Chemical relaxation rates can in principle be obtained provided that the relaxation rate is sufficiently great and that the reaction produces a large change in molecular volume or a large change in refractive increment. In practice, these last two criteria are rarely met (Bloomfield & Lim, 1978).

Many interesting potential applications of QLS to kinetic studies do not fall into either of these limiting categories. We wished to use QLS to monitor changes in protein oligomeric state as a means of testing one model for a mechanism of eukaryotic transcription and replication, but such studies would have to be carried out on the seconds time scale, much faster than possible in a standard QLS experiment.

The DNA of eukaryotes is closely associated with highly conserved histone proteins that fold the DNA in a hierarchical series of stages (van Holde, 1989; Wassarman & Kornberg, 1989; Widom, 1989; Wolffe, 1992). The DNA–histone complex is known as chromatin. In the lowest level of structure, 146 bp long stretches of DNA are locally wrapped in $1^3/_4$ superhelical turns around disk-shaped octameric protein cores that consist of 2 molecules each of histone H2A, H2B, H3, and H4. The resulting particles are known as nucleosome core particles. The enzymes RNA polymerase and DNA polymerase are large in size compared to the histone octamer, yet each must have continuous access to the bases on one strand of the DNA double helix (Widom, 1989). Studies with smaller enzymatic and chemical probes have led to the conclusion that in order for these enzymes to have the necessary access to the DNA bases, the DNA must be removed from the surface of the histone octamer—at least in short stretches—while it interacts with the polymerase enzyme. Despite the great importance of the problem, very little is known about what actually happens on a nucleosome while a polymerase is passing over that stretch of DNA. Indeed,

† This project was supported by grants to J.W. from the NSF and the NIH and by the generous donation of equipment by Hewlett-Packard, Beckman Instruments, Carl Zeiss Inc., Perkin Elmer Cetus, Newport Corp., and Brookhaven Instruments Corp.

* To whom correspondence should be addressed at the Department of Biochemistry, Molecular Biology, and Cell Biology, Northwestern University, 2153 Sheridan Rd., Evanston, IL 60208-3500. Telephone: 708/467-1887. Fax: 708/467-1380.

[1] Abbreviations: QLS, quasielastic light scattering; D_T, translational diffusion coefficient; BSA, bovine serum albumin; BZA, benzamidine hydrochloride; PMSF, phenylmethanesulfonyl fluoride.

0006-2960/93/0432-7824$04.00/0 © 1993 American Chemical Society

at this time, there exist conflicting data in the literature concerning whether the histone octamer is even still bound to DNA after a polymerase has passed by (Bonne-Andrea et al., 1990; Clark & Felsenfeld, 1992; Kirov et al., 1992; Lorch et al., 1987, 1988; Losa & Brown, 1987).

Several models have been put forward for the detailed events involved in the progression of a polymerase over or through nucleosomal DNA (Kornberg & Lorch, 1991, 1992; Thoma, 1991; van Holde et al., 1992). We wish to carry out tests of each of these models. One particularly simple model proposes that the histone octamer may be displaced from the DNA while a polymerase is active at that site and that the octamer then rebinds to that stretch of DNA after the polymerase has passed by. An important attribute of this model is that it allows for maintenance of a relationship between regulatory signals encoded in the form of posttranslational histone modifications (van Holde, 1989; Wassarman & Kornberg, 1989) and the underlying DNA sequence. However, histone octamers are unstable in physiological ionic conditions; at equilibrium, octamers dissociate into an $H3_2H4_2$ tetramer and two H2A–H2B heterodimers (Thomas & Butler, 1977; van Holde, 1989; Wassarman & Kornberg, 1989), and these in turn can repolymerize into nonnative H3–H4 or H2A–H2B polymers (Baxevanis et al., 1991; Royer et al., 1989; Scarlata et al., 1989; Sperling & Bustin, 1975; van Holde, 1989). If histone octamers were to dissociate during the time scale of polymerase progression, they would not be able to re-form a nucleosome after the polymerase had passed by. Strong kinetic traps prevent stepwise reassembly in physiological conditions (van Holde, 1989; Wassarman & Kornberg, 1989), and "instantaneous" complete reassembly would occur with vanishingly low probability because that requires a quaternary reaction. Therefore, one way to test this model for nucleosome transcription is to determine the lifetime of the histone octamer in physiological ionic conditions and to compare this to the time scale for RNA or DNA polymerase to elongate over a distance of one nucleosome, 6–10 s (Shermoen & O'Farrell, 1992).

Continuous-flow methodology has previously been used to allow spectroscopic signal averaging in a kinetically evolving system. Here we report the development of an instrument for continuous-flow QLS that allows diffusion coefficients of kinetically evolving systems to be measured on 1 s or longer time scales while signal-averaging for arbitrarily long periods, as necessary, to achieve a desired signal to noise ratio. Using this instrument, we find that the lifetime of the histone octamer in physiological ionic conditions is <1 s, arguing against a simple model for progression of a polymerase through chromatin. Adaptations of this instrument will extend the range of applicability to time scales shorter than 100 ms.

MATERIALS AND METHODS

Protein Samples. Chicken egg white lysozyme (3× crystallized) and bovine serum albumin (BSA, fraction V) were obtained from Sigma Chemical Co. Prior to use in QLS experiments, they were dissolved in degassed buffer (10 mM Tris, pH 7.5, and 50 mM NaCl) and then centrifuged at 41 000 rpm in a Beckman SW41 rotor at 4 °C for 10–13 h to remove any dust or aggregates.

Histone octamers were isolated from chicken erythrocyte chromatin that was prepared as described (Widom, 1986) with minor modifications. Chromatin was digested with 0.1 Worthington unit of micrococcal nuclease per A_{260} unit of DNA for 16 min at 37 °C to yield predominantly long chromatin fibers, and the digestion was stopped by addition of EDTA to 5 mM. Up to 100 mg of isolated long chromatin

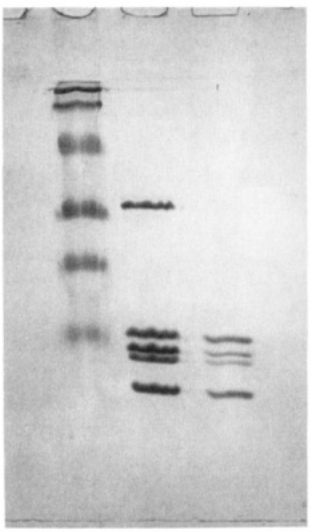

FIGURE 1: Coomassie-stained SDS–polyacrylamide gel. Left, molecular weight standards; center, native long chromatin; right, purified histone octamer. The four core histones which comprise the histone octamer are, in order of decreasing molecular weight, H3, H2B, H2A, and H4.

was then loaded on a 5 cm × 24 cm hydroxylapatite column (Simon & Felsenfeld, 1979; C. Royer, personal communication) that was equilibrated in 0.1 M potassium phosphate, pH 6.7, 0.63 M NaCl, 1 mM BZA, and 0.5 mM PMSF. Elution from the column was monitored by the absorbance at 280 nm (A_{280}). Four or more column volumes of this buffer were used to wash off histones H1 and H5 and any extraneous proteins. Histone octamers were then eluted with 0.1 M potassium phosphate, pH 6.7, 2.0 M NaCl, 1 mM BZA, and 0.5 mM PMSF, the elution continuing until A_{280} returned to base line. DNA was cleaned off the column by extensive washing with 0.5 M potassium phosphate, pH 6.7, 1 mM BZA, and 0.5 mM PMSF, allowing the column to be reused. The purified histone octamer was dialyzed into 10 mM Tris, pH 7.5, 1 mM EDTA, 2.0 M NaCl, 1 mM BZA, and 0.5 mM PMSF and concentrated by vacuum dialysis using a "MicroProDiCon" concentrator (BioMolecular Dynamics) with a PA-15 membrane.

To remove any aggregates produced during the concentration step, or any free histone dimers or tetramers that might possibly be present, the histone octamers were further purified by sucrose gradient centrifugation in linear 5–30% sucrose gradients containing 10 mM Tris, pH 7.5, 1 mM EDTA, 2.0 M NaCl, 1 mM BZA, and 0.5 mM PMSF. The gradients were spun at 4 °C in a Beckman SW-55.1 rotor for 15 h at 55 000 rpm, or in a Beckman SW-41 rotor for 30 h at 41 000 rpm. Gradients were fractionated, and the octamer was located by UV absorption. The gradient-purified histone octamer was then dialyzed into 10 mM Tris, pH 7.5, 1 mM EDTA, 2.0 M NaCl, 1 mM BZA, and 0.5 mM PMSF. The concentration of octamer was determined from A_{276} measured after dilution into 6.0 M guanidine hydrochloride, using an extinction coefficient $\epsilon_{276} = 4.25 \times 10^4\ M^{-1}\ cm^{-1}$ derived from quantitative amino acid analysis, with a molecular weight of 108 585 calculated from the known sequences of the proteins. A Coomassie-stained protein gel of one preparation is shown in Figure 1.

Physical Data. Refractive indexes for the various buffers and protein solutions were measured with a differential refractometer at 23 °C. Solution viscosities were estimated using data from the CRC Handbook of Chemistry and Physics. The (low) protein concentrations were assumed to affect the

solution viscosities negligibly. Viscosity data for 23 °C were estimated from the known values at 20 °C.

RESULTS

Theoretical Considerations. We take advantage of continuous-flow methodology to allow signal-averaging of the autocorrelation function obtained from a narrow window in time in a kinetically evolving system. In a continuous-flow experiment, two reagents are continuously pumped through a mixing device and into and through an observation cell. The reaction of interest is initiated when the two solutions combine in the mixer. Each reagent flow at a constant rate; thus, the mixture flows at a constant rate, and the solution arriving in the observation cell has aged some constant time Δt since the reaction was initiated. For a fixed flow rate and observation point within the observation cell, one can signal-average for as long as desired while acquiring the signal from a constantly replenished reaction mixture maintained at age Δt. In a series of experiments, Δt can be varied over a wide range by changing the flow rate or the distance between the mixer and the observation point, allowing the kinetics of the reaction to be mapped out.

In a continuous-flow QLS experiment, the sample has a uniform flow velocity superimposed on the diffusive motion of the macromolecules. However, this is expected not to alter the autocorrelation function, for two reasons. First, we use the optical homodyne method of detection, and it has been shown theoretically that uniform flow does not contribute to the homodyne autocorrelation function (Berne & Pecora, 1976; Bloomfield & Lim, 1978). Uniform flow can only be detected in a heterodyne experiment. Second, our instrument is designed such that the incident light propagation vector $\mathbf{k}_0$, the scattered light propagation vector $\mathbf{k}_S$, and the flow velocity direction $\mathbf{v}$ are all orthogonal. In a heterodyne experiment, a uniform flow velocity introduces oscillations in the autocorrelation function at the Doppler shift frequency $\Delta\nu = \mathbf{q}\cdot\mathbf{v}/2\pi$, where $\mathbf{q}$ is the scattering vector, given by $\mathbf{k}_0 - \mathbf{k}_S$. Thus, in our instrument, $\mathbf{q}$ is orthogonal to $\mathbf{v}$, and there would be no contribution of flow even to the heterodyne experiment (Berne & Pecora, 1976; Bloomfield & Lim, 1978).

Another potential problem for QLS introduced by flow of the solution arises from the replacement of the correlated scatterers themselves. Replacement of molecules within the scattering volume with new ones at uncorrelated positions provides a mechanism for decay of the correlation function without diffusion. This may be understood most clearly by considering a hypothetical case in which the scatterers diffuse very slowly. In an ordinary QLS experiment, the decay of the autocorrelation function is caused by fluctuations in scattering intensity arising from motion of the scatterers. These fluctuations occur on a characteristic time scale, which is the time required for the scatterers to diffuse a distance comparable to the wavelength of the incident light. If a sample is flowing at a sufficiently high rate, scatterers will be swept out of the scattering volume and replaced with new ones, at uncorrelated positions, before the scatterers have time to diffuse a significant distance (a fraction of the wavelength of the incident light). In this case, the autocorrelation function will still decay over time, but the decay will be due entirely to the flow-induced replacement of the scatterers with uncorrelated ones, with essentially no contribution from diffusion at all. Slower but nonnegligible flow rates could produce a decay time comparable to that due to diffusion, so that an experimentally determined correlation function would artifactually include significant contributions from both diffusion and flow.

The effects of various flow rates on the correlation function can be estimated. A typical diameter for the focused laser beam is 100 μm. We take $\sim$50 μs as a typical time for the scattering intensity autocorrelation function of a diffusing protein in aqueous solution to decay to a few percent of its initial value. A linear flow rate of 10 cm s^{-1} will cause 5% of the molecules within the scattering volume to be replaced with new (uncorrelated) ones during a 50-μs period. Consequently, by the time $\tau \sim 50$ μs ($\tau \equiv$ delay time in the autocorrelation function), there will be a systematic distortion of the normalized correlation function such that its measured value is roughly 5% less than it would be if it were decaying only due to diffusion. At earlier times, when the correlation function has decayed less and is weighted more heavily in model-fitting algorithms, the distortion will be proportionally smaller. Such a modest change in the correlation function might be tolerable, but increasing the flow rate by another factor of 10 would seriously distort the correlation function, rendering the results meaningless. In practice, such flow rates may easily be achieved, and this puts limits on the minimum values of Δt that may be studied, for any particular instrument dead-volume.

Instrumentation. Our QLS instrument is assembled from commercial components and includes: a Coherent Radiation Innova 90-3 argon-ion laser which serves as the light source, operating at 488.0 nm in the TEM_{00} mode with up to 1.3 W of power; a Brookhaven Instruments BI-200 light-scattering goniometer and detector operating in the homodyne mode; and a Brookhaven Instruments BI-2030AT autocorrelator.

The instrument is adapted for the continuous-flow experiments by replacing the standard sample cells with a cell, mixer, and sample delivery system of our own design. An overview of these components is given in Figure 2A, and a detailed drawing of the mixer assembly and flow cell is given in Figure 2B. Reagents are loaded in syringes, with additional reagents loaded in reservoirs that are connected to the system through three-way valves to minimize exposure of reagents to air when refilling the syringes. The reagents are driven into the mixer by two syringe pumps (Orion Research Sage syringe pumps Models 355 and 341B). The mixing ratio and the total flow rate are determined by the speeds of both pumps. After leaving the syringes and outlet valves, the solutions are filtered through 25-mm diameter, 0.45-μm pore-size in-line filters (not shown in illustration) before entering the mixer. A Millex type HV low protein binding filter (Millipore Corp.) is used in the line that contains protein solution; various cellulose acetate or mixed cellulose acetate/nitrocellulose filters are used in the line containing diluent (no protein).

The mixer is made from stainless-steel HPLC fittings. The solutions meet in a T-junction (Upchurch, 1.02-mm i.d. channels) and flow through a short plastic tube to a guard column (Upchurch Model C-130-B) that has a 2 cm long × 2 mm diameter channel filled with glass beads (500-μm diameter) that are held in place with 10-μm stainless-steel frits. Turbulence and variable-length flow paths through the bed of glass beads provide complete mixing. The entire mixer assembly can be siliconized before use, by exposure to dichlorodimethylsilane *in vacuo*. The solution flows from the mixer through a short plastic tube into a three-window fluorescence flow cell (Hellma Model 176.751-QS), with internal dimensions of 3 mm wide × 3 mm deep (back to front) × 11 mm height. The solution enters the observation chamber of the flow cell from the bottom. The cell is positioned in the focused incident laser beam such that the beam is $\sim$2 mm above the bottom of the chamber.

The dead volume of the mixer from the point in the T-junction where the two solutions first meet to the point in the observation cell serving as the scattering volume is

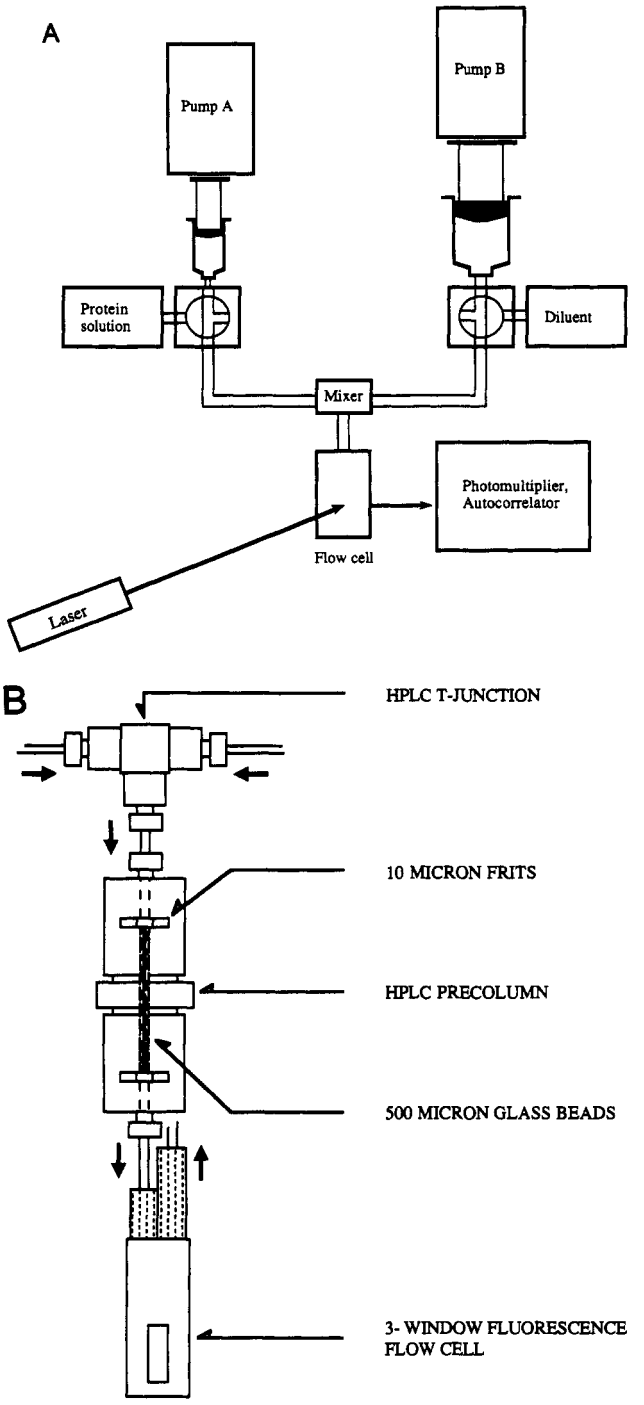

FIGURE 2: (A) Overview of the continuous-flow QLS experiment. (B) Detailed drawing of the mixer and flow cell assembly.

estimated from the known dimensions of each component to be 150 μL. The diameter of the focused laser beam in our instrument is $\sim$100 μm; to avoid significant distortion of the correlation function owing to loss of correlated scatterers as discussed above, we restrict our studies with the present apparatus to Δt values $\geq$1 s. It is helpful in this regard that the linear flow rate through the flow cell is reduced relative to the rate through the tubing by the $\sim$10× larger cross-sectional area inside the flow cell. The deadtime could easily be reduced by reducing the dead volume, which could be accomplished by integrating the components of the mixer into a single unit.

In our initial design, only the flow cell assembly (and the refractive index-matching fluid in which it is immersed) is temperature-regulated. Therefore, we carry out experiments with the room temperature set at 23 °C and controlled to better than ±0.25 °C, and the flow-cell assembly carefully controlled at 23 ± 0.1 °C.

Diluent buffer is degassed under vacuum before being loaded into the syringe and reservoir. Additional buffer corresponding to that present in the protein solution is prepared and degassed, and then the complete solution delivery system and flow cell are extensively flushed until dust and bubbles are eliminated as judged by viewing the scattering volume through a 10× magnifier. Buffer in the sample syringe and reservoir is then withdrawn and replaced with protein solution (upstream of the in-line filter) without allowing air into the line.

To verify the accuracy of the pump flow rate settings, the total flow rate was determined by weighing the effluent of the flow cell delivered into a weighed tube during a known time period. The measured flow rates were in agreement with the expected flow rates to better than ±5%. The relative flow rates of each pump were determined by measuring the concentration of protein before mixing and in the flow cell effluent, using a BCA assay (Pierce) or directly from the UV optical density, and again were found to have their expected values.

We carried out a qualitative assessment of the performance of the mixer by visual inspection of the effluent from mixing a solution of concentrated bromphenol blue dye at pH 7.5 with a diluent of dilute acid. Bromphenol blue turns from an intense dark blue color to a pale yellow/orange upon acidification. We looked for traces or streaks of blue in the effluent, and were unable to detect any. For a more quantitative assessment of mixer performance, the mixer was set up for dilution of a concentrated dye stock. The flow rates were set to yield a delay time in the flow cell of Δt = 1 s after mixing. The flow cell was placed in a spectrophotometer, and the optical density of the flowing solution was monitored at 1-s intervals for a period of 90 s. The optical density of the flowing solution fluctuated during the 90-s runs by ±3.20%.

Model Systems. Control experiments were carried out with two proteins, lysozyme and BSA, to verify that passage of solutions through the mixer as well as flow *per se* did not interfere with measurement of translational diffusion. Autocorrelation functions were accumulated for 30-s intervals while protein solutions were flowing at a rate corresponding to Δt = 2 s; then the pumps were turned off, and further autocorrelation functions were accumulated from the static solution. Translational diffusion coefficients were obtained by fitting the log of the normalized autocorrelation functions using the method of cumulants, and the diameter of the equivalent hydrodynamic sphere (Stokes diameter) was calculated according to the Stokes–Einstein relation. Typical autocorrelation functions and the residuals obtained after fitting are shown in Figure 3, and the calculated Stokes diameters are given in Table I. The quality of the autocorrelation functions and fits under both flowing and static (not flowing) conditions is similar for both proteins, and the resulting Stokes diameters are independent of flow within experimental error.

Histone Octamer. We wished next to use the continuous-flow QLS instrument to determine the lifetime of the histone octamer in physiological ionic strength. Our strategy is to start with a concentrated stock solution of purified histone octamer that is artificially stabilized by the presence of 2.0 M NaCl. This stock solution can then be rapidly mixed with dilute buffer (or, in separate experiments, diluted with additional 2.0 M NaCl), and the diffusion coefficient of the resulting particles can be determined as a function of the time (Δt) after mixing. Histone octamers were prepared from chicken erythrocyte chromatin using hydroxylapatite chro-

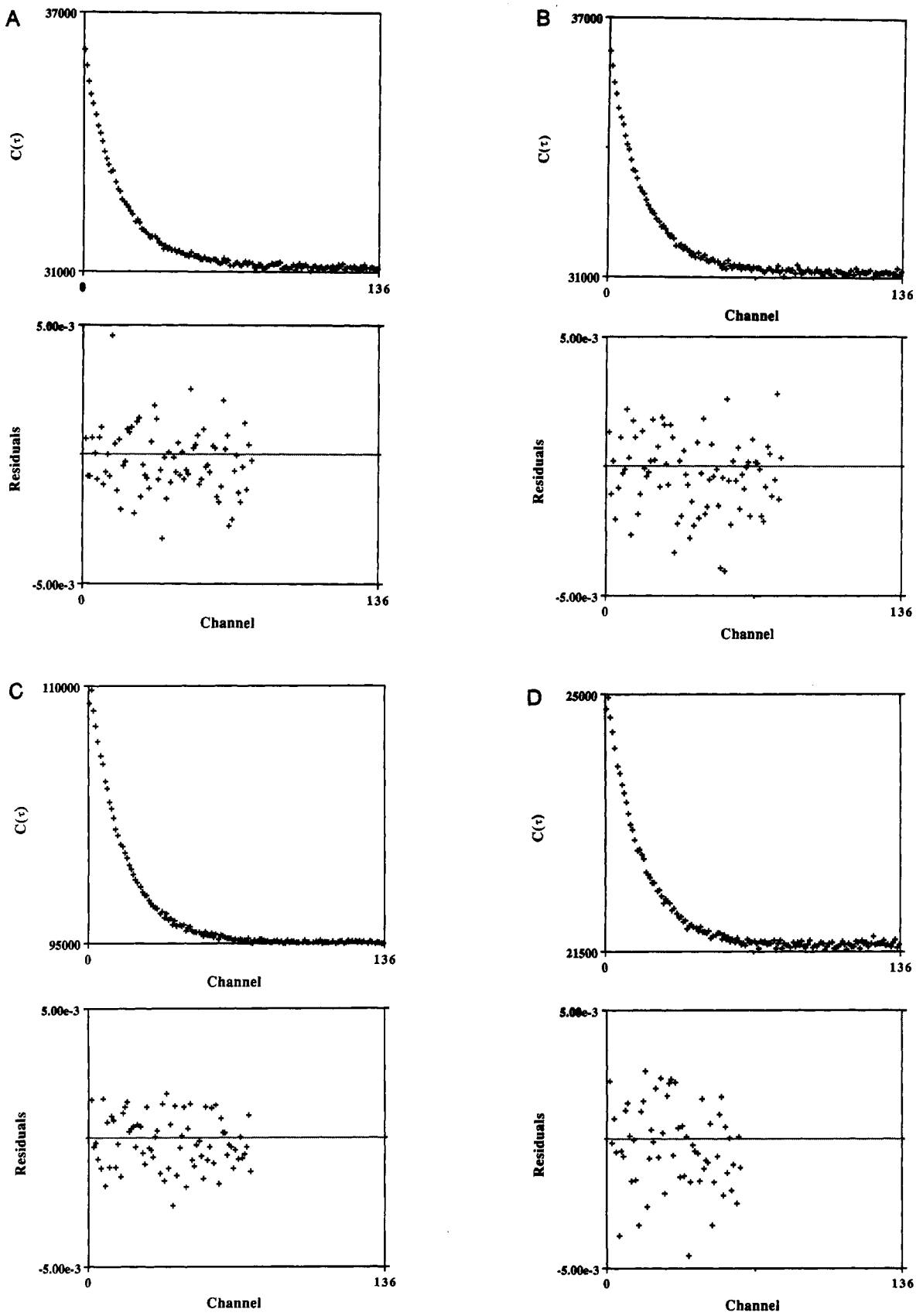

FIGURE 3: Plots of the experimental autocorrelation functions [$C(\tau)$] and residuals after fitting *versus* correlator channel number, for lysozyme (C and D) and BSA (A and B) flowing (B and D) and static (A and C) (not flowing). Correlator time (τ) is given by the channel number times the channel width ($\Delta\tau$). $\Delta\tau$ values of 0.5 and 1.0 μs were used for lysozyme and BSA, respectively. Residuals are defined as the difference between the experimentally determined autocorrelation function (after normalization and base-line-subtraction) and that calculated using the parameters obtained from fitting. Only nonnegative points can be used for fitting the log of the normalized, base-line-subtracted correlation function. To avoid systematic bias, only points for Δt values prior to the first negative point are used for fitting; hence, the residual plots do not extend over all measured correlator channels. Both proteins were dissolved in degassed 10 mM Tris, pH 7.5, and 50 mM NaCl and centrifuged overnight (see Materials and Methods). Lysozyme was studied at 2.0 mg mL^{-1}, and BSA was studied at 0.5 mg mL^{-1}. The temperature of the experiment was controlled at 23 °C; the incident laser light intensity was 1.2 W at 488.0 nm. Accumulation times were 30 s, except for the static lysozyme which was longer, hence the larger number of counts in $C(\tau)$.

Table I[a]

sample	D_{Stokes} (nm)
lysozyme, static	3.70 ± 0.06
lysozyme, flowing	3.76 ± 0.05
BSA, static	7.78 ± 0.08
BSA, flowing	7.78 ± 0.11

[a] T = 23 °C, 10 mM Tris, pH 7.5, 50 mM NaCl. Flow: Δt = 2 s. Error estimates given are the standard deviations for several repetitions.

matography. They were concentrated by vacuum dialysis and then further purified by sucrose gradient ultracentrifugation.

Prior to carrying out the continuous-flow studies, the long-time behavior was investigated by manual mixing. Solutions were allowed to equilibrate for various periods of time at 23 °C and briefly centrifuged to remove dust, and then autocorrelation functions were collected. The autocorrelation functions were analyzed using the method of cumulants. The results for dilution of octamer into buffer containing 2.0 M NaCl were well described by the cumulant fit, and gave a Stokes diameter that was in good agreement with expected values (see below). However, dilution into a final [NaCl] of 0.15 M led to several unexpected results. Analysis of the residuals from cumulant fits revealed systematic deviations of the data from the fits (results not shown). Moreover, the apparent Stokes diameter obtained from the fits increased with the time of equilibration over a time scale of tens of minutes, ultimately reaching values that were significantly in excess of that determined for the octamer itself. It is known that the H2A–H2B heterodimers and the $H3_2H4_2$ tetramers produced by dissociation of histone octamers can form unnatural aggregates in approximately physiological ionic strength (Baxevanis et al., 1991; Royer et al., 1989; Scarlata et al., 1989; Sperling & Bustin, 1975; van Holde, 1989). We suspected that some of the heterodimers or tetramers or both might be polymerizing over time and that the autocorrelation functions obtained included contributions from both aggregates and any remaining heterodimers and tetramers.

To examine this hypothesis, autocorrelation functions obtained for histone octamer diluted into 2.0 M NaCl or into 0.15 M NaCl were subjected to size-distribution analysis using the computer program NNLS (Brookhaven Instruments; Morrison et al., 1985). This program finds the distribution of particle sizes among a set of exponentially spaced particle sizes that minimizes the squares of the deviation between the calculated autocorrelation function and the experimental data ("least squares"), subject to the important physical constraint that all coefficients of the distribution (intensity-weighted relative concentrations) must be nonnegative.

The results from one such experiment are given in Figure 4. For octamer diluted into 2.0 M NaCl, the NNLS distribution analysis reveals a single component, and the peak of the distribution occurs at a Stokes diameter equal to that obtained using the cumulant fit. However, the results for dilution into 0.15 M NaCl are quite different. We consistently find that the size distribution for octamer diluted into 0.15 M NaCl includes a predominant component having a Stokes diameter of ~5 nm, together with a smaller amount of material having a much larger size, which must reflect the presence of aggregated material. Note that the intensity-weighting inherent in a QLS experiment implies that only a small fraction of all particles have those large sizes. The presence of such aggregates explains both the failure of the cumulant fit to adequately describe the data and the unexpectedly large apparent size that is determined when the cumulant fit is used. We therefore used NNLS to analyze the results for the octamer dilution experiments described below. The Stokes

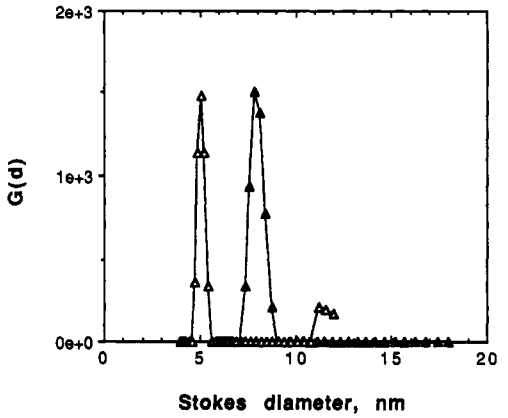

FIGURE 4: NNLS size distribution analysis for histone octamer diluted into 2.0 M NaCl (▲) or 0.15 M NaCl (△). $G(d)$ is the intensity-weighted distribution of scatterers having Stokes diameter = d. All solutions additionally contained 10 mM Tris, pH 7.5, 1 mM EDTA, 1 mM BZA, and 0.5 mM PMSF. T = 23 °C; $[octamer]_{final}$ = 0.54 mg mL^{-1}; incident light intensity = 1.0 W at 488.0 nm; accumulation time = 100 s. The first 128 autocorrelator channels were divided into 4 groups of 32 each, that were assigned channel widths ($\Delta\tau$) of 1, 1, 2, and 4 μs, respectively.

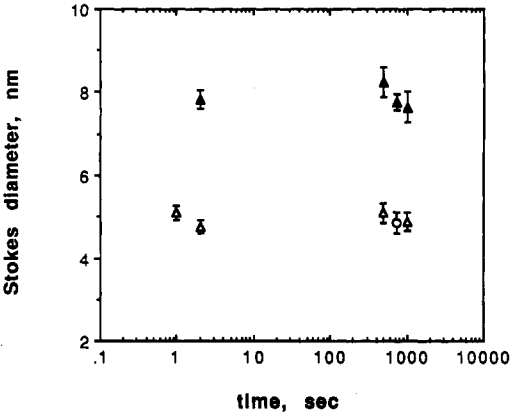

FIGURE 5: Stokes diameters for histone octamer diluted into 2.0 M NaCl (▲), 0.15 M NaCl (△), or 0.10 M NaCl (○) measured as a function of time after mixing. All solutions additionally contained 10 mM Tris, pH 7.5, 1 mM EDTA, 1 mM BZA, and 0.5 mM PMSF. T = 23 °C; $[octamer]_{final}$ = 0.54, 0.36, or 0.29 mg mL^{-1}; incident light intensity = 1.3 W at 488.0 nm. The first 128 autocorrelator channels were divided into 4 groups of 32 each, that were assigned channel widths ($\Delta\tau$) of 1, 1, 2, and 4 μs, respectively. Time points at 500, 750, and 1000 s were obtained by manual mixing, and were accumulated for 100 s. Time points at 1.0 and 2.0 s were obtained by continuous-flow, using total flow rates (of the mixed solution) of 9.0 and 4.5 mL min^{-1}, respectively. For the continuous-flow experiments, the pumps were run for 15 s (to establish steady-state flow rates) prior to the start of 30-s-long accumulations.

diameters presented are those pertaining to the predominant, unaggregated component for the 0.15 M NaCl data, or for the single component present for the 2.0 M NaCl data.

Octamer dilution studies were carried out for delay times (Δt) after dilution of 1.0, 2.0, 500, 750, and 1000 s. Delay times of 1.0 and 2.0 s were obtained using the continuous-flow technique, and the longer delay times were prepared by manual mixing. The octamer concentration after dilution was 0.54 or 0.29 mg mL^{-1} for jumps to 2.0 and 0.15 M NaCl, and 0.36 mg mL^{-1} for the jumps to 0.1 M NaCl. Each experiment was repeated several times, from each of two different preparations of octamer. The results are shown in Figure 5. Error bars represent the standard deviations between the repeated measurements.

Dilution of octamer to 2.0 M NaCl, conditions in which the octamer remains intact (Philip et al., 1979; Thomas & Butler, 1977; van Holde, 1989), leads to a Stokes diameter of 7.87

± 0.26 nm, whether measured at early times (Δt = 2 s) in the continuous-flow experiment or at longer times after manual mixing. However, dilution of octamer into physiological ionic strength (0.15 M NaCl) or slightly lower (0.1 M NaCl), conditions in which the octamer is not stable for extended periods of time, yields a much smaller Stokes diameter, 4.93 ± 0.15 nm, even by the earliest time investigated, Δt = 1 s. It is expected that the Stokes diameter of H2A–H2B heterodimers and $H3_2H4_2$ tetramers will be sufficiently close that NNLS may not be able to resolve them, particularly if data are slightly noisy. Moreover, it is known that octamers in physiological ionic strength do dissociate completely into these small oligomers, at least after relatively long time (Philip et al., 1979; Thomas & Butler, 1977; van Holde, 1989). Therefore, we expect that the single peak (of unaggregated material) in the NNLS size distribution for octamer diluted into 0.15 or 0.10 M NaCl may represent the intensity-weighted average distribution for a mixture containing these H2A–H2B heterodimers and $H3_2H4_2$ tetramers.

Hydrodynamic Simulations. The true hydrodynamic size of the histone octamer is not known with certainty. A relatively wide range of measured sedimentation coefficients and partial specific volumes have previously been reported (van Holde, 1989). One study (Philip et al., 1979) reports that the sedimentation coefficient depends strongly on the rotor speed (presumably a result of a pressure-dependent equilibrium constant), and reports data for a range of rotor speeds extrapolated to zero. Using the data reported in that study ($s_{20,w}$ = 6.6 S, partial specific volume v_2 = 0.73 cm^3 g^{-1}), we calculate a Stokes diameter of 7.9 nm, in good agreement with that determined here.

A lower bound on the Stokes diameter of the histone octamer can be calculated from the structure determined by X-ray crystallography (Arents et al., 1991; Richmond et al., 1984). The structure approximates that of a wedge-shaped disk: viewed from one perspective, it appears circular in outline, with a diameter of 6.5 nm, and viewed from an orthogonal direction, it appears wedge-shaped, with a minimum thickness of 1.0 nm and a maximum thickness of 6.0 nm. We have carried out a computer simulation of the translational frictional coefficient for this complex shape, to estimate the Stokes diameter. This shape for the octamer was represented on a cubic lattice with 0.10-nm lattice spacing. A total of 108 596 small spheres having radii of 0.05 nm were appropriately positioned to describe the shape. The frictional coefficient for this assembly of spheres was evaluated by computer, using standard methods (Cantor & Schimmel, 1980; Draves et al., 1992; Yao et al., 1990, 1991). We calculate that the Stokes diameter of this assembly is 6.03 nm. Importantly, however, only 70% of the protein is visible in the structure at its present resolution (Arents et al., 1991). One or more of the "tails" of each polypeptide chain are believed to be extended and disordered, and are not visible in the map. Hence, the wedge-shaped disk represents a lower bound on the true size of the octamer. If an additional 30% of the octamer mass were assumed to be added as a spherical shell around this equivalent hydrodynamic sphere, this would increase the Stokes diameter to 6.8 nm; if some of the extra mass were extended into solution, as is believed to be the case, rather than added as a spherical shell, this would readily account for the Stokes diameter of 7.9 nm measured here and by Philip et al. (1979).

We have not attempted to carry out detailed hydrodynamic calculations for the mixture of H2A–H2B heterodimer plus $H3_2H4_2$ tetramer that would correspond to fully dissociated histone octamer. However, we have made an estimate for a simple model in which the octamer is represented as eight equal-sized spheres, hexagonally packed in a three-dimensional cluster; the tetramer is represented as four of these spheres packed in a tetrahedron, and each of the heterodimers is represented as two spheres in contact. For this simple model, the intensity-weighted average Stokes diameter for the dissociated oligomers is computed to be 0.71 times the Stokes diameter of the intact octamer, or ~5.6 nm. This value is somewhat larger than the 4.9-nm average diameter that we measure experimentally, but considering the simplicity of the model, the agreement is fair. Moreover, since the small amount of aggregate present is likely to be enriched in—or exclusively composed of—the (larger) $H3_2H4_2$ tetramers (Baxevanis et al., 1991; Royer et al., 1989; Scarlata et al., 1989), the mixture contributing to the peak in the distribution at 4.9 nm may be relatively enriched for the (smaller) H2A–H2B heterodimers, leading to a smaller than expected average diameter.

We conclude that our measured Stokes diameter for the octamer in 2.0 M NaCl, 7.87 ± 0.26 nm, is appropriate for that structure and that the measured Stokes diameter in 0.15 and 0.10 M NaCl, 4.93 ± 0.15 nm, is substantially too low for it to have come from an intact histone octamer. These data imply that the histone octamer has dissociated into its component smaller oligomers when diluted into physiological ionic strength and, importantly, that this dissociation is complete by the earliest time for which we have obtained data, Δt = 1 s.

DISCUSSION

Continuous-Flow QLS. A chief conclusion of this work is that continuous-flow QLS experiments are feasible. The present apparatus allows measurements of D_T to be made for time scales (Δt) ≥1 s after mixing, with negligible distortion of the autocorrelation function. The flow rate necessary for Δt = 1 s is approximately 9 mL min^{-1} of the mixed solution. For small proteins such as lysozyme, final protein concentrations (after mixing) of 2 mg mL^{-1} yield usable autocorrelation functions after ~30 s of accumulation. For larger proteins or oligomeric assemblies, substantially lower final protein concentrations suffice.

The present system is assembled from commercially available components, and has a dead volume of approximately 150 μL. It should be straightforward to integrate the mixer and flow cell into a single custom-fabricated unit, thereby reducing the dead volume by a factor of ~10. This would allow measurements to be made for Δt values as short as ~100 ms, with no other modifications to the system. A 10-fold decrease in the system dead volume would offer the additional important benefit of decreasing by 10-fold the total amount of protein consumed during an experiment for any particular value of Δt.

For any particular system dead volume, it should also be possible to extend the capabilities to shorter Δt by explicitly correcting for the distortions to the autocorrelation function caused by flow. The distortion in $C(\tau)$ due to flow could be calculated if the diameter of the focused laser beam in the scattering volume and the linear flow rate of the sample through the beam were known. Alternatively, slowly diffusing scatterers could be used to measure directly the distortion in $C(\tau)$ due to flow.

Test of a Mechanism for Nucleosome Transcription. A second chief conclusion from this study pertains to the lifetime of the histone octamer and its relationship to mechanisms of nucleosome transcription. We find that, when exposed to physiological ionic strength in the absence of DNA, histone octamers dissociate into their component H2A–H2B heterodimers and $H3_2H4_2$ tetramers on a time scale faster than 1 s after mixing, the earliest time point that we could

investigate. With one caveat, discussed below, this result argues against one simple model for the progression of RNA or DNA polymerase through chromatin. Typical elongation rates for eukaryotic RNA or DNA polymerases are ~23 nucleotides s^{-1} (Shermoen & O'Farrell, 1992). The minimum value for the length of DNA associated with and protected by the histone octamer is the 146 bp of the nucleosome core particle, and thus the time scale during which a polymerase interacts with this length of DNA is ~6 s, significantly longer than our upper limit on the lifetime of the histone octamer. We conclude that it is not the case that histone octamers could simply dissociate from their DNA while a polymerase is resident and then rebind to their original locations after the polymerase has passed by.

A criticism of this experiment is that the histone octamers start out artificially stabilized by the presence of 2.0 M NaCl, rather than naturally stabilized by being bound to 146 bp of DNA. The possibility exists that the artificially stabilized histone octamer has undergone some conformational transition already, and therefore has a shorter lifetime in physiological ionic conditions than would a histone octamer that had just been pushed off of its DNA by a polymerase. This was a necessary compromise for us to make in order for the experiment to be carried out. Importantly, however, the structure of histone octamer that was artificially stabilized in high ionic strength conditions has been determined by X-ray crystallography (Arents et al., 1991), and is found to be very similar in size and shape to that of the histone octamer in the nucleosome core particle, also determined by X-ray crystallography (Richmond et al., 1984). Thus, there is no indication that the artificially stabilized octamer has undergone some destabilizing pretransition.

Many other models for the fate of histone octamers during transcription or replication are not tested by this experiment, and must await future investigation. It remains possible that histone octamers are *not* fully displaced from the DNA while a polymerase passes by. It is also possible that octamers *are* fully displaced from their starting location on the DNA but that, rather than remaining free in solution for the full time of polymerase progression while they await the opportunity to rebind at their starting location (during which time, as the present study demonstrates, they would dissociate), the octamers could instead diffuse on a very rapid time scale to a new location on a stretch of bare DNA behind the polymerase. Experimental evidence in support of this model has recently been reported (Clark & Felsenfeld, 1992). However, it is not clear that such behavior applies *in vivo*. One would expect many histone octamers to diffuse in the wrong direction, because of the stochastic nature of diffusion; moreover, except for special cases such as ribosomal genes, electron microscopic images of transcribing chromatin fail to reveal the presence of nucleosome-sized stretches of bare DNA behind RNA polymerase (Foe et al., 1976).

If histone octamers are fully released from the DNA and are not immediately transferred to bare DNA behind the polymerase, then the present study implies that the octamers will dissociate into H2A–H2B heterodimers and $H3_2H4_2$ tetramers. In this case, after the polymerase has passed by and a histone octamer is reassembled on this stretch of DNA, it follows that the reassembled octamer would be composed of *scrambled* components. We note that biochemical evidence of such scrambling associated with transcription and replication has been reported (Jackson, 1990).

ACKNOWLEDGMENT

We thank Anna Camarena for her assistance with an early stage of this work, Cathy Royer for advice concerning the purification of histone octamers, and Peggy Lowary for helpful discussions and comments on the manuscript.

REFERENCES

Aksiyote-Benbasat, J., & Bloomfield, V. A. (1975) *J. Mol. Biol. 95*, 335–337.
Aksiyote-Benbasat, J., & Bloomfield, V. A. (1981) *Biochemistry 20*, 5018–5025.
Arents, G., Burlingame, R. W., Wang, B.-C., Love, W. E., & Moudrianakis, E. N. (1991) *Proc. Natl. Acad. Sci. U.S.A. 88*, 10148–10152.
Baxevanis, A. D., Godfrey, J. E., & Moudrianakis, E. N. (1991) *Biochemistry 30*, 8817–8823.
Berne, B. J., & Pecora, R., Eds. (1976) in *Dynamic Light Scattering*, p 376, John Wiley & Sons, Inc., New York.
Bloomfield, V. A., & Lim, T. K. (1978) *Methods Enzymol. 48*, 415–494.
Bonne-Andrea, C., Wong, M. L., & Alberts, B. M. (1990) *Nature 343*, 719–726.
Cantor, C. R., & Schimmel, P. R., Eds. (1980) in *Biophysical Chemistry*, W. H. Freeman, San Francisco.
Chu, B. (1974) in *Laser Light Scattering*, p 317, Academic Press, Inc., Orlando.
Clark, D. J., & Felsenfeld, G. (1992) *Cell 71*, 11–22.
Draves, P. H., Lowary, P. T., & Widom, J. (1992) *J. Mol. Biol. 255*, 1105–1121.
Foe, V. E., Wilkinson, L. E., & Laird, C. D. (1976) *Cell 9*, 131–146.
Jackson, V. (1990) *Biochemistry 29*, 719–731.
Kirov, N., Tsaneva, I., Einbinder, E., & Tsanev, R. (1992) *EMBO J. 11*, 1941–1947.
Kornberg, R. D., & Lorch, Y. (1991) *Cell 67*, 833–836.
Kornberg, R. D., & Lorch, Y. (1992) *Annu. Rev. Cell Biol. 8*, 563–587.
Lorch, Y., LaPointe, J. W., & Kornberg, R. D. (1987) *Cell 49*, 203–210.
Lorch, Y., LaPointe, J. W., & Kornberg, R. D. (1988) *Cell 55*, 743–744.
Losa, R., & Brown, D. D. (1987) *Cell 50*, 801–808.
Morrison, I. D., Grabowski, E. F., & Herb, C. A. (1985) *Langmuir*, 496–501.
Pecora, R., Ed. (1985) *Dynamic Light Scattering*, 420 pp, Plenum Press, New York.
Philip, M., Jamaluddin, M., Sastry, R. V. R., & Chandra, H. S. (1979) *Proc. Natl. Acad. Sci. U.S.A. 76*, 5178–5182.
Richmond, T. J., Finch, J. T., Rushton, B., Rhodes, D., & Klug, A. (1984) *Nature 311*, 532–537.
Royer, C. A., Rusch, R. M., & Scarlata, S. F. (1989) *Biochemistry 28*, 6631–6637.
Scarlata, S. F., Ropp, T., & Royer, C. A. (1989) *Biochemistry 28*, 6637–6641.
Shermoen, A. W., & O'Farrell, P. H. (1992) *Cell 67*, 303–310.
Simon, R. H., & Felsenfeld, G. (1979) *Nucleic Acids Res. 6*, 689–696.
Sperling, R., & Bustin, M. (1975) *Biochemistry 14*, 3322–3331.
Thoma, F. (1991) *Trends Genet. 7*, 175–177.
Thomas, J. O., & Butler, P. J. G. (1977) *J. Mol. Biol. 116*, 769–781.
van Holde, K. E. (1989) in *Chromatin* (Rich, A., Ed.) p 497, Springer-Verlag, New York.
van Holde, K. E., Lohr, D. E., & Robert, C. (1992) *J. Biol. Chem. 267*, 2837–2840.
Widom, J. (1986) *J. Mol. Biol. 190*, 411–424.
Widom, J. (1989) *Annu. Rev. Biophys. Biophys. Chem. 18*, 365–395.
Wolffe, A., Ed. (1992) in *Chromatin Structure and Function*, Academic Press, London.
Yao, J., Lowary, P. T., & Widom, J. (1990) *Proc. Natl. Acad. Sci. U.S.A. 87*, 7603–7607.
Yao, J., Lowary, P. T., & Widom, J. (1991) *Biochemistry 30*, 8408–8414.